第 48 卷 第 11 期
2021 年 11 月

湖南大学学报（自然科学版）
Journal of Hunan University（Natural Sciences）

Vol. 48 No. 11
November 2021

Open Access Article

Stress-Strain Relationship of High-Performance Concrete in Compression

Alan S. Habib, Omar Q. Aziz

Civil Engineering Department, University of Salahaddin-Erbil, Kurdistan Region, Iraq

Abstract: The application of High-Performance Concrete (HPC) technology has grown considerably in the construction industry due to the advantages associated with its mechanical properties and durability of concrete. The stress-strain model of concrete is essential in the design stage of structural members. Since the development of HPC, the behaviors of many stress-strain models for HPC have been predicted to be different from each other due to the different mix proportions and material properties. This unique study utilizes a comparison exclusively between three different strengths of HPC at different ages to produce the stress-strain curve. Many stress-strain curves are available, but no research has been conducted on comparing three different stress-strain curves of HPC in compression, so this study aims to do that. In this study, an experimental technique (compressometer) is used to generate the stress-strain curves of HPC in compression with the compressive strengths of approximately 40, 60, and 80 MPa mixes 1, 2, and 3, respectively. The compressive strength variation was obtained by varying the water to binder ratio of the mix, addition of silica fume, superplasticizer (PC200), and the age of testing. It was observed that at the maximum strain of $2x10^{-3}$, the compressive strength of mix2 is increased by 21.4% compared to mix1, mix3 has increased by 9.8% compared to mix2, and finally, mix3 has increased by 29.1% compared to mix1. The consequence of these variables on the shape of stress-strain curves is presented and discussed.

Keywords: compression, high performance concrete, silica fume, strain, stress.

高性能混凝土受壓時的應力-應變關係

摘要：高性能混凝土技術的應用在建築行業得到了長足的發展，因為它具有與混凝土機械性能和耐久性相關的優勢。混凝土的應力應變模型在結構構件的設計階段是必不可少的。自高性能混凝土發展以來，由於混合比例和材料特性的不同，高性能混凝土的許多應力-應變模型的行為被預測為彼此不同。這項獨特的研究專門對不同年齡的三種不同強度的高性能混凝土進行比較，以生成應力-應變曲線。許多應力-應變曲線可用，但沒有研究比較壓縮中高性能混凝土的三種不同應力-應變曲線，因此本研究旨在做到這一點。在本研究中，使用實驗技術（壓縮計）生成壓縮強度約為 40、60 和 80兆帕的混合 1、2 和 3 的高性能混凝土的應力-應變曲線。通過改變混合物的水與粘合劑的比例、添加矽粉、超塑化劑 (个人电脑200) 和測試年齡來獲得抗壓強度變化。觀察到在最大應變為 $2x10^{-3}$ 時，混合2 的抗壓強度比混合1 提高了 21.4%，混合3 比混合2 提高了 9.8%，最後，混合3 比混合1 提高了 29.1%。介紹並討論了這些變量對應力-應變曲線形狀的影響。

关键词：壓縮、高性能混凝土、矽粉、應變、應力。

1. Introduction

High-Performance Concrete (HPC) is the well-known construction material for structural application providing greater advantages such as durability and longer life than traditional normal strength concrete (NSC). Demand for HPC increased compared to past decades since the dimensions of member sections can be reduced even further in buildings [1-3]. According to ACI committee 363, HPC is concrete that possesses high workability, strength, and high durability which certain characteristics are developed for a particular application and environment. HPC is concrete that meets special combinations of performance and uniformity requirements that cannot always be

Received: July 24, 2021 / Revised: September 1, 2021 / Accepted: October 3, 2021 / Published: November 30, 2021

About the authors: Alan S. Habib, Omar Q. Aziz, Civil Engineering Department, University of Salahaddin-Erbil, Kurdistan Region, Iraq

achieved routinely using conventional constituent materials and normal mixing, placing, and curing practices [19]. HPC is usually characterized by its' special performance and uniformity in both the short and long term [9, 16]. When considering concrete as a structural material, compressive strength becomes an essential parameter required for the ultimate strength design of various structural members. Generally, nonlinear analysis is used to study the structural members' failure response in which the compressive Stress-Strain curves are considered the main basis of design [10, 11, and 15]. Many pieces of research and investigations have been carried out to represent the stress-strain relationship of HPC by using standard mathematical curves, for example, a parabola, hyperbola, ellipse, cubic parabola, or combinations like a parabola with a straight line or a sine wave with a cubic parabola [4, 5, and 6]. In order to obtain a full stress-strain curve, a special technique is required due to the brittleness of HPC. For instance, the axial deformation has been used for test control but for HPC, the large energy release at the time of failure causes an unstable descending branch [7]. In order to overcome this problem, the circumferential deformation can be used as suggested by [8] or the combination of axial load and axial deformation. Many equations for HPC stress-strain curves have been developed, and Table 1 shows some of the proposed equations. In this research, attempts will be made to get acceptable concrete strains for the entire stress-strain curve.

2. Materials and Methods

2.1. Material Properties

- Ordinary Portland cement was used in this investigation, CEM-I 42.5R mass cement, produced in Kurdistan/Iraq.
- The type of silica fume used was micro silica Supaflo – MS90.
- HPC superplasticizer (Supaflo PC200) to obtain a workable concrete having a low water/binder ratio under ASTM C494-Type A & G.
- Crushed natural coarse aggregate with a maximum aggregate size of 9.5 mm.
- River sand under ASTM specifications.
- Ordinary drinking water was used for mixing and curing all kinds of concrete.

2.2. Mix Design Proportions

Mixing of materials was done in a rotary mixer having a capacity of 0.1 m^3; the materials (gravel & sand) were dry mixed for 3-5 minutes. Then the mixture of pre-mixed silica Fume and cement was added to the aggregates, and the mixer started to mix for additional 3-5 minutes. After that, the pre-mixed water with superplasticizer was added gradually with continuous mixing for about three more minutes to react with the binders. Table 2 illustrates the details of the designed mix proportions.

2.3. Casting and Curing

For the compressive strength test of concrete, 9 cylindrical specimens (150 x 300 mm) were cast for each mix under ASTM C31 [18]. The specimens were stripped from the molds after 24 hours and cured in water in a controlled room having a temperature of approximately 20℃ for 7, 28, and 56 days. The samples were then removed prior to testing, air-dried for a few hours, and capped according to ASTM C 617 [20] to have a smooth and leveled surface to ensure the uniform distribution of the compressive load between cylinders and machine, as shown in Fig. 1.

Table 1 Existing stress-strain models for high strength concrete [13, 14]

Authors (year)	Model description	Parameter description	strength range (MPa)	Author's remarks
Single model capable of predicting stress-strain response from the origin to ultimate (i.e., $0 < \varepsilon \le \varepsilon_u$).				
Sargin and Handa (1969)	$\frac{f_c}{f'_c} = k_3 \frac{A\left(\frac{\varepsilon_c}{\varepsilon'_c}\right) + (D-1)\left(\frac{\varepsilon_c}{\varepsilon'_c}\right)^2}{1 + (A-2)\left(\frac{\varepsilon_c}{\varepsilon'_c}\right) + D\left(\frac{\varepsilon_c}{\varepsilon'_c}\right)^2}$	$A = \frac{E_{it}}{E_c}$; $D = 0.65 - 7.25f'_c \times 10^{-3}$ $E_{it} = 5979\sqrt{f'_c}$; $\varepsilon'_c = 0.0021$	-	
Popovics (1973)	$\frac{f_c}{f'_c} = \frac{\beta\left(\frac{\varepsilon_c}{\varepsilon'_c}\right)}{\beta - 1 + \left(\frac{\varepsilon_c}{\varepsilon'_c}\right)^\beta}$	$\beta = .058f'_c + 1$	Up to 51	
Wang *et al.* (1978)	$\frac{f_c}{f'_c} = \frac{A(\varepsilon_c/\varepsilon'_c) + B(\varepsilon_c/\varepsilon'_c)^2}{1 + C(\varepsilon_c/\varepsilon'_c) + D(\varepsilon_c/\varepsilon'_c)^2}$	A, B, C and D are constants which can be estimated by considering the condition A $\left\{\begin{matrix} \frac{f_c}{f'_c} = 0.45 \text{ for } \varepsilon_c/\varepsilon'_c = \frac{0.45}{E_{it}/E_c} \\ \frac{f_c}{f'_c} = 1 \quad \text{for} \quad \varepsilon_c/\varepsilon'_c = 1 \end{matrix}\right\}$	Up to 76	
Carreira and Chu (1985)	$\frac{f_c}{f'_c} = \frac{\beta(\varepsilon_c/\varepsilon'_c)}{\beta - 1 + (\varepsilon_c/\varepsilon'_c)^\beta}$	$\beta = \frac{1}{1 - (\frac{f'_c}{\varepsilon'_c E_{it}})}$ $E_{it} = \frac{f'_c}{\varepsilon'_c}\left(\frac{24.82}{f'_c} + 0.92\right)$ $\varepsilon'_c = (1{,}680 + 7.1\, f'_c) \times 10^{-6}$	23 to 80	Does not fit on current data, due to negative value of β
Two models, one for combine prediction of the behavior of rising branch and falling branch up to the limiting strain (i.e., $0 < \varepsilon \le \varepsilon_{c,lim}$), while the second model predicts the behavior of the depressing branch from limiting strain up to the ultimate strain (i.e., $\varepsilon_{c,lim} < \varepsilon \le \varepsilon_u$).				
CEB-FIP Model Code 90 (1993)	For $0 \le \varepsilon \le \varepsilon_{c,lim}$ $f_c = f'_c \frac{\left(\frac{E_{it}}{E_c}\right)\left(\frac{\varepsilon_c}{\varepsilon'_c}\right) - \left(\frac{\varepsilon_c}{\varepsilon'_c}\right)^2}{1 + \left(\frac{E_{it}}{E_c} - 2\right)\left(\frac{\varepsilon_c}{\varepsilon'_c}\right)}$ For $\varepsilon > \varepsilon_{c,lim}$ $f_c = \frac{f'_c}{\left(\frac{\xi}{\eta_2} - \frac{2}{\eta_2^2}\right)\left(\frac{\varepsilon_c}{\varepsilon'_c}\right)^2 + \left(\frac{4}{\eta_2} - \xi\right)\left(\frac{\varepsilon_c}{\varepsilon'_c}\right)}$	$\frac{\varepsilon_{c,lim}}{\varepsilon'_c} = \frac{1}{2}\left[\left(\frac{E_{it}}{2E_c} + 1\right) + \sqrt{\left(\frac{E_{it}}{2E_c} + 1\right)^2 - 2}\right]$ $\eta_2 = \frac{\varepsilon_{c,lim}}{\varepsilon'_c}$ $\xi = 4\frac{\eta_2^2\left(\frac{E_{it}}{E_c} - 2\right) + 2\eta_2 - \frac{E_{it}}{2E_c}}{\left[\eta_2\left(\frac{E_{it}}{2E_c} - 2\right) + 1\right]^2}$	Up to 90	Modified form of Sargin and Handa (1969)
Hsu and Hsu (1994)	For $0 \le \varepsilon \le \varepsilon_{c,lim}$ $\frac{f_c}{f'_c} = \frac{n\beta(\varepsilon_c/\varepsilon'_c)}{n\beta - 1 + (\varepsilon_c/\varepsilon'_c)^{n\beta}}$ For $\varepsilon > \varepsilon_{c,lim}$ $f_c = 0.3f'_c e^{-0.8\left(\frac{\varepsilon_c}{\varepsilon'_c} - \frac{\varepsilon_{c,lim}}{\varepsilon'_c}\right)^{0.5}}$	$\beta = \left(\frac{f'_c}{65.23}\right)^3 + 2.59$ where, $E_{it} = 0.0736w^{1.51}(f'_c)^{0.3}$, $\varepsilon_o = (1680 + 7.1f'_c) \times 10^{-6}$ For $0 \le \varepsilon \le \varepsilon'_c$; n=1 For $\varepsilon'_c \le \varepsilon \le \varepsilon_d$; n=1 if $f'_c < 62$ MPa n=2 if 62 MPa $< f'_c < 76$ MPa n=3 if 76 MPa $< f'_c < 90$ MPa n=5 if $f'_c \ge 90$ MPa $\varepsilon_{c,lim}$ is the strain at $0.3f'_c$ in the falling branch of stress-strain curve	> 69	The expression is the modified form of Carreira and Chu (1985)
Van Gysel and Taerwe (1996)	For $0 \le \varepsilon \le \varepsilon_{c,lim}$ $f_c = f'_c \frac{\left(\frac{E_{it}}{E_c}\right)\left(\frac{\varepsilon_c}{\varepsilon'_c}\right) - \left(\frac{\varepsilon_c}{\varepsilon'_c}\right)^2}{1 + \left(\frac{E_{it}}{E_c} - 2\right)\left(\frac{\varepsilon_c}{\varepsilon'_c}\right)}$ For $\varepsilon > \varepsilon_{c,lim}$ $f_c = \frac{f'_c}{\left(\frac{\xi}{\eta_2} - \frac{2}{\eta_2^2}\right)\left(\frac{\varepsilon_c}{\varepsilon'_c}\right)^2 + \left(\frac{4}{\eta_2} - \xi\right)\left(\frac{\varepsilon_c}{\varepsilon'_c}\right)}$	$\frac{\varepsilon_{c,lim}}{\varepsilon'_c} = \frac{1}{2}\left[\left(\frac{E_{it}}{2E_c} + 1\right) + \sqrt{\left(\frac{E_{it}}{2E_c} + 1\right)^2 - 2}\right]$ $\eta_2 = \frac{\varepsilon_{c,lim}}{\varepsilon'_c}$ $\xi = 4\frac{\eta_2^2\left(\frac{E_{it}}{E_c} - 2\right) + 2\eta_2 - \frac{E_{it}}{2E_c}}{\left[\eta_2\left(\frac{E_{it}}{2E_c} - 2\right) + 1\right]^2}$	Up to 90	The expression is the modified form of CEB-FIP Model Code 90 (1993)
Lu and Zhao (2010)	For $0 \le \varepsilon \le \varepsilon_L$ $\frac{f_c}{f'_c} = \left[\frac{(E_{it}/E_c)(\varepsilon_c/\varepsilon'_c) - (\varepsilon_c/\varepsilon'_c)^2}{1 + (E_{it}/E_c - 2)(\varepsilon_c/\varepsilon'_c)}\right]$ For $\varepsilon > \varepsilon_d$ $\frac{f_c}{f'_c} = \frac{1}{1 + \lambda[(\varepsilon_c/\varepsilon'_c) - 1/(\varepsilon_L/\varepsilon'_c) - 1]^{2(1-\lambda)}}$	$\varepsilon_L = \varepsilon'_c\left[\left(\frac{1}{10}\frac{E_{it}}{E_c} + \frac{4}{5}\right) + \sqrt{\left(\frac{1}{10}\frac{E_{it}}{E_c} + \frac{4}{5}\right)^2 - \frac{4}{5}}\right]$ where, ε_L is the strain at $0.8f'_c$ in the falling branch of stress-strain curve	50-140	For $0 \le \varepsilon \le \varepsilon_L$, modified form of Sargin and Handa (1969) and for $\varepsilon > \varepsilon_L$, model of Van Gysel and Taerwe (1996) is used

Fig. 1 Capping of the specimens

2.4. Testing of Specimens

As soon as the curing period was completed, all 27 cylinders (9 for each group) were tested using a Universal Testing Machine (UTM) having a capacity of more than 2000 kN. The compressive test was carried out in 7, 28, and 56 days under ASTM C39 [17]. During the test, a compressometer with a dial-gauge was used to determine the strain and deformation characteristics of the concrete specimens, as shown in Fig. 2. The results of the tested specimens are tabulated in Table 3.

Fig. 2 Compressometer with a dial gauge

Table 2 Mix design proportions

Mix No.	Mix proportion C:S:G by weight	Water/Cement ratio	Silica fume	Admixture/ Cement	Target compressive strength MPa
1	1:1.33:2.67	0.42	-	-	40
2	1:1.2:1.8	0.30	4%	1.6%	60
3	1:1.5:2.36	0.28	14%	1.2%	80

Table 3 Test results of compression, stress at peak strain Ec, f_r and concrete density γ_c of all specimens

Mix No.	Age (Days)	f'c (MPa)	Ec (GPa)	Stress at peak strain of $2x10^{-3}$ (MPa)	Modulus of rupture f_r (MPa)	γ_c at 56 days (Kg/m^3)
	7	36	-	-	2.07	-
Mix 1	28	43.3	30.82	35.9	4.72	-
	56	45.8	33.3	44.73	6.13	2462
	7	43.95	-	-	3.88	-
Mix 2	28	60.54	33.1	54.5	6.34	-
	56	69.6	35.93	56.92	7.5	2483
	7	55.17	-	-	8.02	-
Mix 3	28	70.91	36.35	58.1	10.28	-
	56	75.56	39.6	63.1	11.05	2509

3. Results and Discussion

3.1. Compressive Strength (f'c)

In this study, three different mixes were used to obtain f 'c of approximately (40, 60 and 80) MPa and were tested at three different ages; the results of the tested samples can be seen in Table 3. Fig. 3 shows the relation between the compressive strength and age for the 40 MPa set of samples. It can be noted that the compressive strength at 7 days reached 36 MPa, which is about 90% of its designed strength which is about 15% more than what is expected to reach at 7 days (60-75 %), and it reaches its designed strength at 28 days as at 56 days passes its designed strength.

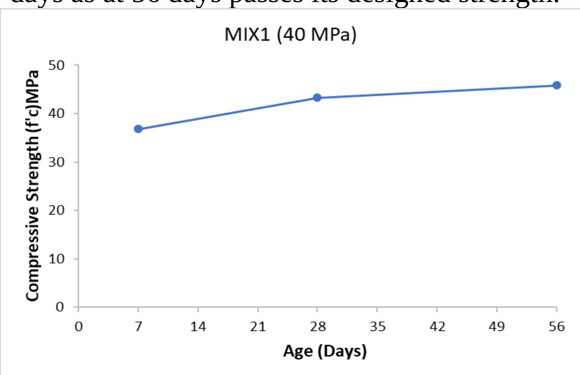

Fig. 3 Compressive strength progression of 40 MPa at different ages

For the second set of samples, which is 60 MPa shown in Fig. 4, the compressive strength reaches approximately 73% of its designed strength in b7 days and 100% of its designed strength in 28 days, and finally, just over 100% in 28 days.

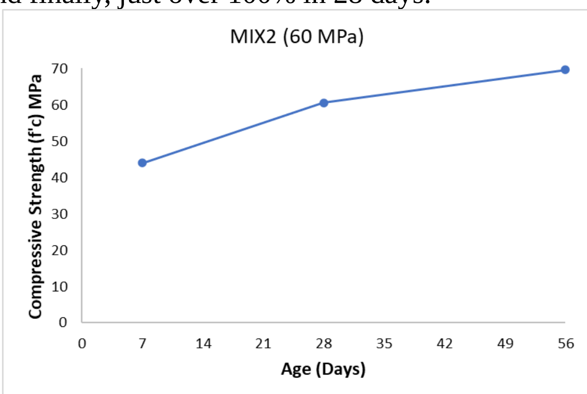

Fig. 4 Compressive strength progression of 60 MPa at different ages

For the third set of samples, which is 80 MPa as illustrated in Fig. 5, the obtained compressive strength was close to 69% of its total strength in 7 days and approximately 89% of its total strength in 28 days, whereas, in 56 days, it reached about 95% of its designed strength. In high strength concrete, the chemical reaction which causes the hydration sometimes could go on up to 90 days (but at a slower rate compared to the progress from 7 to 28 days) to reach the desired strength, and this deficit in total strength after 56 days could be the case with this mix.

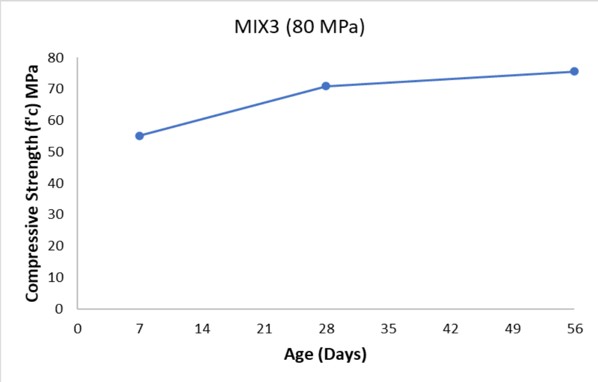

Fig. 5 Compressive strength progression of 80 MPa at different ages

Fig. 6 illustrates the differences in compressive strength in all three mixes after 7 days. It can be observed that the compressive strength of mix2 is approximately 16.3% greater than mix1; consequently, the strength of mix3 is about 20.4% greater than that of mix2.

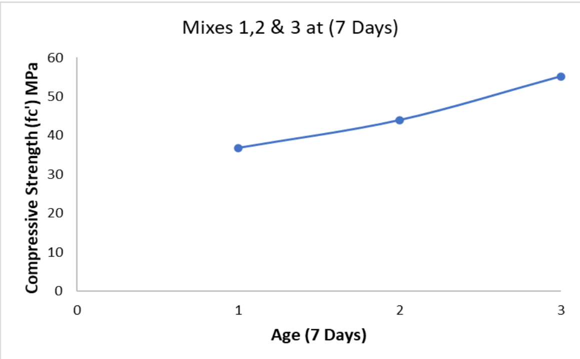

Fig. 6 Compressive strength of all three mixes at 7 days

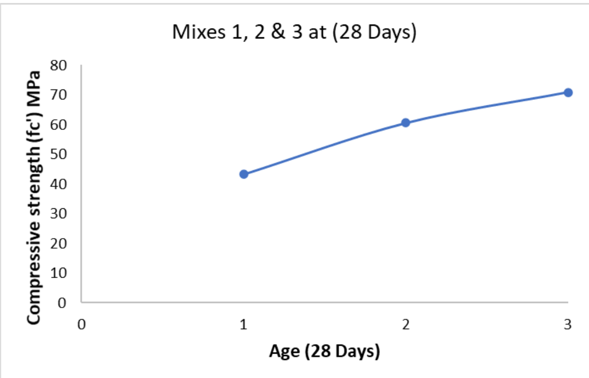

Fig. 7 Compressive strength of all three mixes at 28 days

The differences in compressive strength for all three mixes after 28 days are shown in Fig. 7. As can be seen, the compressive strength of mix2 is 28.5% greater than mix1, whereas the strength of mix3 is 14.6% greater than that of mix2.

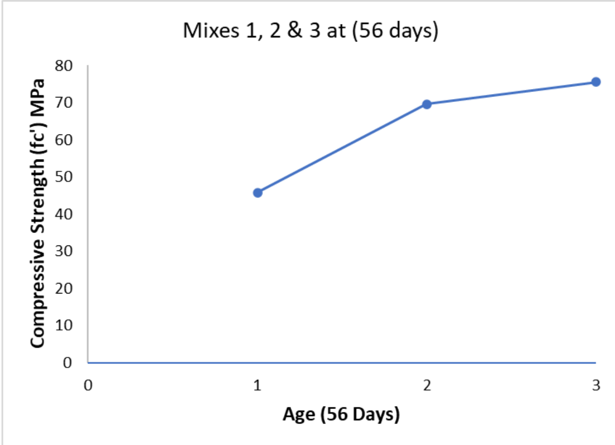

Fig. 8 Compressive strength of all three mixes at 56 days

The differences in compressive strength for all three mixes after 56 days are illustrated in Fig. 8. The compressive strength obtained from mix2 is 34.2% greater than mix1, whereas the strength of mix3 is 7.9% greater than that of mix2. It can be noted that the percentage increase between mixes 1 & 2 is considerably higher than that of mixes 2 & 3, this is because of the addition of (silica fume) in mixes 2 & 3 and mixes 2 & 3 are considered as High Strength Concrete in which they require 56 days to reach its potential strength while mix 1 reached its potential strength at 28 days.

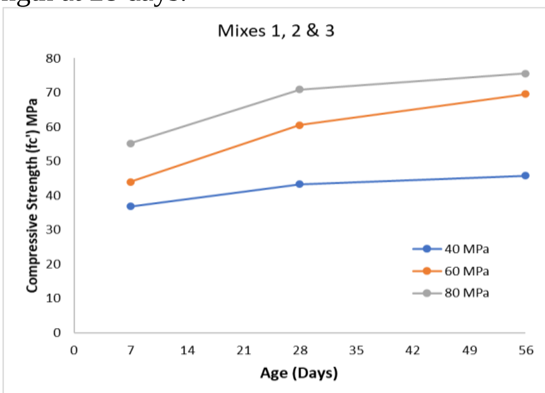

Fig. 9 Progression in compressive strength of all three mixes at different ages

Fig. 9 shows the progression of compressive strength of all three mixes at different ages. It can be observed that mix1 reaches its maximum strength at 28 days, and the increase in strength after 28 days is extremely slow, which is expected as it does not contain any admixtures. The difference in strength becomes obvious between mixes 1&2 and mixes 1&3 after 28 days because of the introduction of admixtures such (superplasticizer and silica fume). Also, the differences between mixes 2 & 3 are due to the amount of each admixture in the mix and, most importantly, the differences in water/cement ratio in each mix, as shown in Table 2.

3.2. Stress-Strain Relationship

The key parameters usually used to characterize a stress-strain curve: compressive strength f‘c, initial tangent modulus, and stress at peak strain Ec obtained from the laboratory are presented in Table 3.

It can be seen from all (stress-strain) curves for all mixes that the maximum strain values do not go past $2x10^{-3}$ due to the removal of the compressometer instrument in order to prevent the compressometer from being damaged. Also, it can be seen from Figs. 11-15 that for HPC, the shape of the ascending part of the stress-strain curve is more linear and steeper, increasing elastic modulus, and the peak strain is significantly higher than conventional concrete, which is investigated by Aguirre [12] as sown in Fig. 10.

Fig. 11 shows the stress-strain curve of mix1 at 28 and 56 days, having a compressive strength of 43.3 and 45.8 MPa, respectively. During measuring the stress-strain curve, at the maximum strain of $2x10^{-3}$, the compressive strength was recorded as 35.9 and 44.73 MPa for 28 and 56 days, respectively. It is clear that for 28 days, the maximum strain of $2x10^{-3}$ was reached at the stress of 35.9, whereas at the same stress for 56 days, the strain was recorded to be $1.2x10^{-3}$ and the difference in compressive stress between 28 and 56 days at maximum strain was recorded as 19.7%.

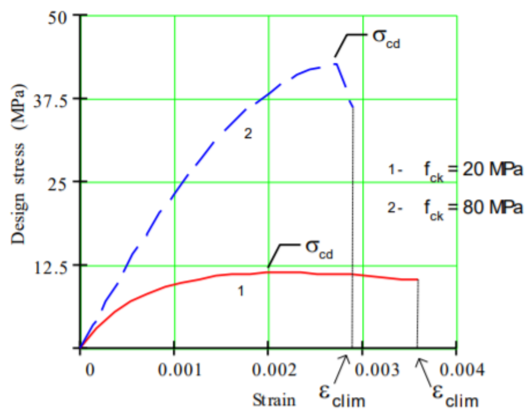

Fig. 10 Design stress-strain curves of HPC and conventional concrete by Aguirre

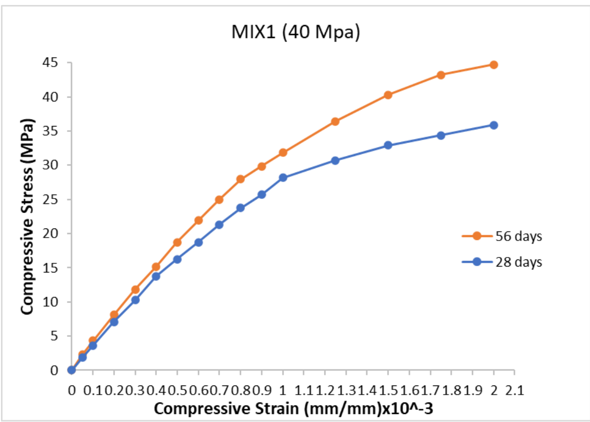

Fig. 11 Compressive (stress vs. strain) curve of mix1 (40 MPa) at 28 & 56 days

From Fig. 12, the compressive strength of mix2 at 28 and 56 days was recorded as 60.54 and 69.6 MPa, respectively. During the test and at the maximum strain of $2x10^{-3}$, when taking measurements at the time of testing, the stress of 54.5 and 56.92 MPa were taken for 28 and 56 days, respectively. It can be observed that for 28 days, the maximum strain of $2x10^{-3}$ was reached at the stress of 54.5, whereas at the same stress for 56 days, the strain was taken as $1.7x10^{-3}$ and the difference in compressive stress between 28 and 56 days at maximum strain was calculated as 4.25%.

For mix3 having a compressive strength of 75.56 at 56 days, the maximum strain of $2x10^{-3}$ was reached at 63.1 MPa as shown in Fig. 13, and at 28 days for the same strain, the compressive stress was recorded as 58.1 MPa and the difference in compressive stress between 28 and 56 days at maximum strain was calculated as 7.9%.

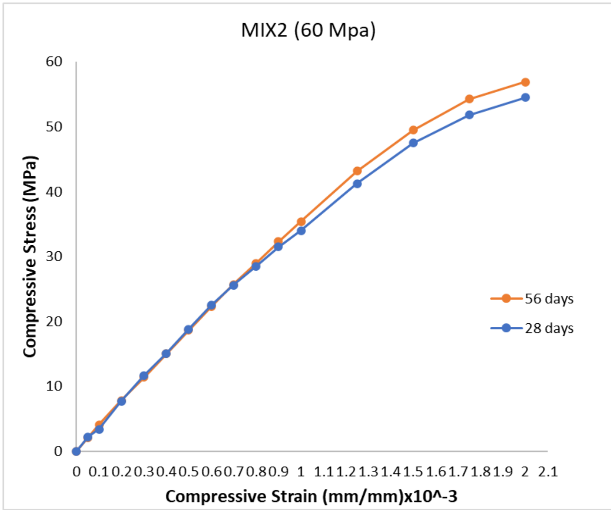

Fig. 12 Compressive (stress vs. strain) curve of mix2 (60 MPa) at 28 & 56 days

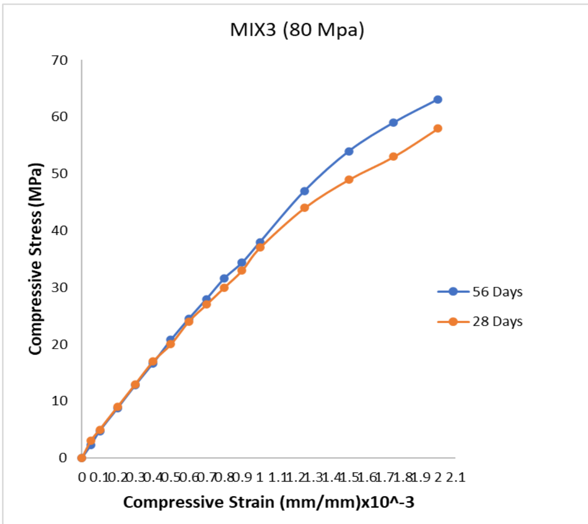

Fig. 13 Compressive (stress vs. strain) curve of mix3 (80 MPa) at 28 & 56 days

Fig. 14 shows the stress-strain curve of mixes 1, 2 & 3 at 28 days, having a compressive strength of 43.3, 60.54 & 70.91 MPa, respectively. During the test, at the maximum strain of $2x10^{-3}$, the compressive strength was taken to be 35.9 MPa, 54.5 MPa, and 58.1 MPa for mixes 1, 2 & 3, respectively.

It can be seen that mix1 reached a maximum strain of $2x10^{-3}$ at the stress of 35.9 MPa, whereas mix2 at the same stress only reached $1.1x10^{-3}$ and mix3 reached $0.9x10^{-3}$. It is obvious from the curves that the compressive strength of mix2 is greater than mix1 by 34%, and mix3 is greater than mix1 and mix2 by 38% and 6%, respectively, at the maximum strain of $2x10^{-3}$.

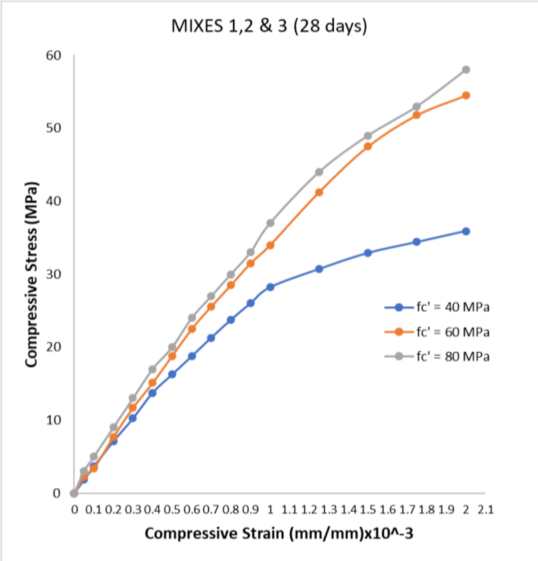

Fig. 14 Compressive (stress vs. strain) curve of mixes 1, 2 & 3 at 28 days

Fig. 15 shows the stress-strain curve of mixes 1, 2, and 3 at 56 days, having a compressive strength of 45.8, 69.6, and 75.56 MPa, respectively. However, at the maximum strain of $2x10^{-3}$, the stresses recorded were 44.73, 56.92, and 63.1 MPa for mixes 1, 2, and 3, respectively. From the curve, it can be observed that mix1 reached a maximum strain of $2x10^{-3}$ at the stress of 44.73 MPa, whereas mix2 and mix3 at the same stress only reached $1.3x10^{-3}$ and $1.2x10^{-3}$, respectively. At maximum strain of $2x10^{-3}$, the compressive strength of mix2 is increased by 21.4% compared to mix1, mix3 has increased by 9.8% compared to mix2, and finally, mix3 has increased by 29.1% compared to mix1.

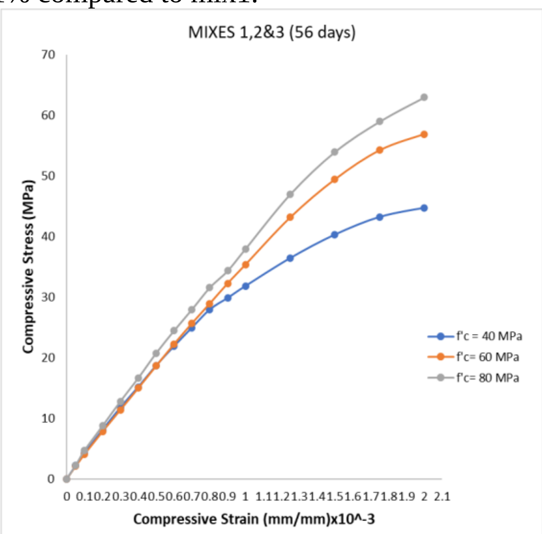

Fig. 15 Compressive (Stress vs. Strain) curve of all mixes at 56 days

4. Conclusion

To date, many pieces of research and investigations have been conducted on the stress-strain relationship in compression using various materials such as steel fiber, fly ash (FA), slag (SL), steel fiber with different percentages in the resulting concrete. However, very few concentrated on using silica fume with superplasticizer with different ratios in the mix and compared three different concrete strengths at different concrete ages.

When HPC is used, it is essential to study stress-strain diagrams having more accurate characteristics for this material. Codes regulating this material have realistic curves permitting a more suitable design to fit the experimental results. The traditional procedures developed for the conventional concrete have to be improved for HPC design. Advantages of the potential of HPC could be achieved by enhancing the current design procedures.

The following conclusions can be drawn based on the test results and cross-comparisons:

1) It can be noted that the compressive strength of concrete is considerably influenced by the use of superplasticizer (Supaflo PC200) and silica fume, when the percentage of silica fume increased by 10% in mix3, the compressive strength increased whereas, when the superplasticizer decreased by 0.4% resulted to an increase in compressive strength.

2) The effect of water/cement ratio on compressive strength can be seen clearly in the three designed mixes in such a way that when the W/C decreased from 0.42 to 0.30 for mix2 and 0.28 for mix3, the compressive strength increased in each case.

3) The stress-strain curve was drawn based on the results obtained from experimental work using three different mixes to get (40, 60, and 80) MPa, each with its specific proportions of materials and different ratios of admixture in a way that when the percentage of silica fume increased by 4% and 14% for mixes 2 and 3, the mixes became more ductile.

4) The effect of compressive strength is obvious from all the stress-strain curves drawn; as compressive stress increased, the compressive strain decreased in different mixes and different ages as can be seen from the results, mix3 recorded less strain compared to mix2 and mix1 at any given stresses; also, mix2 recorded less strain compared to mix1 at any given stresses.

5) At maximum strain of $2x10^{-3}$, the compressive strength of mix2 is increased by 21.4% compared to mix1, mix3 has increased by 9.8% compared to mix2, and finally, mix3 has increased by 29.1% compared to mix1.

Though quite good results have been observed, it is essential to study more percentage replacement of OPC silica fume and superplasticizer and also need to study the durability performance of HPC to draw a strong conclusion. This project is an ongoing one; further work is currently underway.

Acknowledgment

The authors acknowledge the cooperation and support provided by the Concrete and Structures Lab of Salahaddin University/College of Engineering.

References

[1] LIAO W., PERCEKA W., and LIU E. Compressive stress-strain relationship of high strength steel fiber reinforced concrete. *Journal of Advanced Concrete Technology*, 2015, 13: 379-392.

[2] MOSTOFINEJAD D., and NOZHATI M. Prediction of the modulus of elasticity of high strength concrete. *Iranian Journal of Science & Technology*. *Transaction B, Engineering*, 2005, 29(B3).

[3] VAN GYSEL A., and TAERWE L. Analytical formulation of the complete stress-strain curve for high strength concrete. *Materials and Structures*, 1996, 29(9): 529-533.

[4] AZIZ O.Q. and ABDUL-AHAD, R.B. Stress-Strain curves of fibrous concrete in compression. *Journal of Zankoy Sulaimany – Part A*, 2002, 5(2). DOI: https://doi.org/10.17656/jzs.10096

[5] AZIZ O.Q., and TAHA B.O. Mechanical properties of High Strength Concrete (HSC) with and without chopped carbon fiber (CCF). *International Journal of Civil Engineering*, 2013, 2 (2): 1-12.

[6] BAALBAKI W., AITCIN P. C., and BALLIVY G. On predicting modulus of elasticity in high-strength concrete. ACI Materials Journal, 1992, 89(5): 517-520.

[7] VAN MIER JGM, SHAH SP, ARNAUD M., BALAYSSAC J.P., BASCOUL A., CHOI S., DASENBROCK D., FERRARA G., FRENCH C., GOBBI M.E., KARIHALOO B.L., KÖNIG G., KOTSOVOS M.D., LABUZ J., LANGE-KORNBAK D., MARKESET G., PAVLOVIC M.N., SIMSCH G., THIENEL K.-C., TURATSINZE A., ULMER M., VAN GEEL H.J.G.M., VAN VLIET M.R.A., and ZISSOPOULOS D. Strain-softening of concrete in uniaxial compression. *Materials and Structures*, 1997, 30: 195-209. https://doi.org/10.1007/BF02486177

[8] JANSEN D.C., SURENDRA P.S., and ROSSOW E.C. Stress-strain results of concrete from circumferential strain feedback control testing. *Materials Journal*, 1995, 92(4): 419-428.

[9] CUSSON D., and PAULTRE P. Stress-Strain model for confined high strength concrete. *Journal of Structural Engineering*, 1993, 121(3): 468-477.

[10] LU Z.H., and ZHAO Y.G. Empirical stress-strain model for unconfined high-strength concrete under uniaxial compression. *Journal of Materials in Civil Engineering*, 2010, 22(11): 1181-1186.

[11] GUTIERREZ P.A., and CANOVAS M.F. The Modulus of elasticity of High-Performance Concrete. materials and structures, 1995, 28(184): 559-568.

[12] FRANCISCO A.T. Axial load and moment interaction charts for High Performance Concrete. *Investigación y Desarrollo*, 2003, 1(3): 29-41.

[13] SHAFIQ N., AYUB T., and NURUDDIN M. Predictive Stress-Strain models for High Strength Concrete subjected to uniaxial compression. *Applied Mechanics and Materials*, 2014, 567: 476-481. DOI:10.4028/www.scientific.net/AMM.567.476.

[14] SHAFIQ N., AYUB T., and NURUDDIN M. Stress-strain response of High Strength Concrete and application of the existing models. *Research Journal of Applied Sciences, Engineering, and Technology*, 2014, 8(10): 1174-1190. DOI:10.19026/rjaset.8.1083.

[15] HSU L., and HSU C.T. Complete stress-strain behavior of high-strength concrete under compression. *Magazine of Concrete Research*, 1994, 46(169): 301-312.

[16] MIAH M.J., MIAH M.S., UDDIN M.A., and SUZAUDOULA M. Optimization of mechanical properties of high performance concrete made with fly ash and blast furnace slag. In: *4th International Conference on Advances in Civil Engineering*, 2018.

[17] ASTM. *C39/C39M Standard Test Method for Compressive Strength of Cylindrical Concrete Specimens*. West Conshohocken, PA, USA, 2018.

[18] ASTM. *C31/C31M Standard Practice for Making and Curing Concrete Test Specimens in the Field*. West Conshohocken, PA, USA, 2019.

[19] AMERICAN CONCRETE INSTITUTE. *ACI 318-19M: Building Code Requirements for Structural Concrete and Commentary*. ACI Committee 318, Farmington Hills, MI, USA, 2019.

[20] ASTM. *C617 / C617M-15 Standard Practice for Capping Cylindrical Concrete Specimens*. West Conshohocken, PA, USA, 2015.

参考文:

[1] LIAO W., PERCEKA W., 和 LIU E. 高強度鋼纖維混凝土的壓縮應力-應變關係。先進混凝土技術雜誌，2015，13：379-392。

[2] MOSTOFINEJAD D., 和 NOZHATI M. 高強混凝土彈性模量的預測。伊朗科學技術雜誌。交易乙，工程，2005，29(乙3)。

[3] VAN GYSEL A. 和 TAERWE L. 高強度混凝土完整應力-應變曲線的分析公式。材料與結構，1996 年，29(9)：529-533。

[4] AZIZ O.Q. 和 ABDUL-AHAD, R.B. 纖維混凝土受壓時的應力-應變曲線。贊科伊·蘇萊曼尼雜誌——一个部分，2002 年，5(2)。DOI：https://doi.org/10.17656/jzs.10096

[5] AZIZ O.Q. 和 TAHA B.O. 含有和不含短切碳纖維的高強度混凝土的機械性能。國際土木工程雜誌, 2013, 2 (2): 1-12.

[6] BAALBAKI W.、AITCIN P. C. 和 BALLIVY G. 關於預測高強度混凝土的彈性模量。美國混凝土協會材料雜誌，1992，89(5)：517-520。

[7] VAN MIER J.G.M., SHAH S.P., ARNAUD M., BALAYSSAC J.P., BASCOUL A., CHOI S., DASENBROCK D., FERRARA G., FRENCH C., GOBBI M.E., KARIHALOO B.L., KÖNIG G., KOTSOVOS M.D., LABUZ J.、LANGE-KORNBAK D.、MARKESET G.、PAVLOVIC M.N.、SIMSCH

G.、THIENEL K.-C.、TURATSINZE A.、ULMER M.、VAN GEEL H.J.G.M.、VAN VLIET M.R.A. 和 ZISSOPOULOS D. 拉緊-混凝土在單軸壓縮下的軟化。材料與結構，1997，30：195-209。 https://doi.org/10.1007/BF02486177

[8] JANSEN D.C.、SURENDRA P.S. 和 ROSSOW E.C. 圓周應變反饋控制測試中混凝土的應力-應變結果。材料雜誌, 1995, 92(4): 419-428。

[9] CUSSON D. 和 PAULTRE P. 約束高強度混凝土的應力-應變模型。結構工程雜誌, 1993, 121(3): 468-477。

[10] 陸振華, 趙永光.單軸受壓無側限高強混凝土的經驗應力-應變模型。土木工程材料學報, 2010, 22(11): 1181-1186.

[11] GUTIERREZ P.A. 和 CANOVAS M.F. 高性能混凝土的彈性模量。材料與結構，1995，28(184): 559-568。

[12] FRANCISCO A.T. 高性能混凝土的軸向載荷和力矩相互作用圖。調查開發, 2003, 1(3): 29-41。

[13] SHAFIQ N.、AYUB T. 和 NURUDDIN M. 單軸壓縮下高強度混凝土的預測應力-應變模型。應用力學與材料，2014，567：476-481。DOI：10.4028/www.scientific.net/AMM.567.476。

[14] SHAFIQ N.、AYUB T. 和 NURUDDIN M. 高強度混凝土的應力應變響應和現有模型的應用。應用科學、工程與技術研究學報，2014，8(10): 1174-1190. DOI:10.19026/rjaset.8.1083。

[15] HSU L. 和 HSU C.T. 受壓下高強混凝土的完全應力-應變行為。混凝土研究雜誌，1994，46（169）：301-312。

[16] MIAH M.J.、MIAH M.S.、UDDIN M.A. 和 SUZAUDOULA M. 用粉煤灰和高爐礦渣製成的高性能混凝土的力學性能優化。在：第四屆土木工程進展國際會議，2018。

[17]美國測試與材料協會。C39/C39米圓柱混凝土試樣抗壓強度的標準測試方法。美國賓夕法尼亞州西康紹霍肯，2018 年。

[18]美國測試與材料協會。C31/C31米現場製作和固化混凝土試樣的標準操作規程。美國賓夕法尼亞州西康紹霍肯，2019 年。

[19] 美國混凝土協會。国际交流协会318-19米：結構混凝土的建築規範要求和註釋。美國混凝土協會委員會 318，美國密歇根州法明頓希爾斯，2019 年。

[20] 美國測試與材料協會。C617/C617米-15 圓柱形混凝土試樣封蓋的標準做法。美國賓夕法尼亞州西康紹霍肯，2015 年。